Int. J. Solids Structures Vol. 19, No. 3, pp. 207–228, 1983
Printed in Great Britain.

0020-7683/83/030207-22$03.00/0
Pergamon Press Ltd.

GLOBAL-LOCAL LAMINATE VARIATIONAL MODEL

N. J. PAGANO
AFWAL/MLBM, Wright-Patterson AFB, OH 45433, U.S.A.

and

S. R. SONI
University of Dayton Research Institute, Dayton, OH 45469, U.S.A.

(*Received* 9 *December* 1981)

Abstract—The absence of a unified, tractable model to predict the elastic response of a multi-layered laminate (say 100 layers) has foiled attempts to understand the failure modes of practical composite structures. Global models, which follow from an assumed displacement field and lead to the definition of effective (or smeared) laminate moduli, are not sufficiently accurate for stress field computation. On the other hand, local models, in which each layer is represented as a homogeneous anisotropic continuum, become intractable as the number of layers becomes even moderately large (approx. 10). In this work, we blend these concepts into a self-consistent model which can define detailed response functions in a region of interest (local), while representing the remainder of the domain by effective properties (global). In this investigation the laminate thickness is divided into two parts. A variational principle has been used to derive the governing equations of equilibrium. For the global region of the laminate, potential energy has been utilized, while the Reissner functional has been used for the local region. The field equations are based upon an assumed thickness distribution of stress components within each layer of the local region and displacement components in the global region. The derived boundary conditions imply that the computed stress field on the surfaces of the global region and the prescribed tractions (point wise in an elasticity sense) satisfy the conditions of vanishing resultant force and moment identically. The same conditions are satisfied in the local region. The stress fields obtained by this formulation compare very well with those obtained by other approaches for laminates with a small number of layers. For large number of layers, internally consistent results are achieved by varying the representation of the global region in the present model.

INTRODUCTION

The principal problem of interest in the present investigation is the same as that treated in [1], i.e. the stress analysis of a composite laminate built of anisotropic elastic layers of uniform thickness and subjected to prescribed tractions and/or displacements on its boundary surfaces. The body is bounded by a cylindrical edge surface and upper and lower faces that are parallel to the interfacial planes. This assumption is made only for convenience in writing the governing equations. There is no difficulty in extending the model to include laminates of variable thickness.

In practical applications, numerous layers may be present (use of 100 layers in aircraft structures is not unusual). Contemporary models are incapable of providing precise resolution of the local stress fields in the vicinity of stress raisers under such conditions. Global models, which follow from an assumed, usually elementary, displacement field, lead to the definition of effective (or smeared) laminate moduli and are not sufficiently accurate for stress field computation [1]. On the other hand, local models, in which each layer is represented as a homogeneous, anisotropic continuum, become intractable as the number of layers becomes even moderately large—in some methods as few as four layers result in technical/economic barriers to accurate stress resolution. In this work we blend these concepts into a self-consistent model which can define detailed response functions in a particular, predetermined region of interest (local), while representing the remainder of the domain by effective properties (global). Such dual representations are not without precedent in solid mechanics. For example, Gurtin [2] discussed this approach with reference to the solution of crack-tip stress field problems. Wang and Crossman [3] used an effective modulus representation of regions of a laminate, however, only the extensional response of the regions were considered, i.e. the flexural and flexural-extension coupling characteristics of laminated bodies were ignored. Hence, that approach fails to provide correct solutions to certain elementary laminate problems for which exact solutions are available. Stanton *et al.* [4] used a global representation based upon a three dimensional laminate model developed by Pagano [5] which is based upon the assumption that the stress field is only a function of one space coordinate. This is a generalization and improvement of the material model given in [3], however, this approach is not convenient for coupling with the model presented earlier [1]. Furthermore, it is desirable to retain the model [6] as a special degenerate case of a global model since that result was shown to produce very good agreement with a known elasticity solution for transverse normal stress σ_z [7].

There have been several investigations of the interlaminar stress fields in laminated composites. Pagano [1] has given a detailed description of the relevant literature in this field. A recent review article [8] by Solomon presents an up to date literature survey in related topics as of 1980. In the present paper, reference will be made of only those publications which are not covered by [1, 8]. Spilker and Ting [9] have conducted the static and dynamic analysis of composite laminates using hybrid stress finite elements. Raju *et al.* [10] have investigated the free edge stresses in layered plates using eight node isoparametric elements. In both these publications, the laminate idealization for a reasonably accurate finite element analysis had to be very fine, i.e. a quarter of the laminate was divided into about 600 elements. No more than four layers were considered for numerical calculations. For moderately large number of plies (say 10), these approaches will lead to computer storage/economic difficulties.

Blumberg *et al.* [11] studied the edge effects and stress concentrations in composite laminates made of glass sheets bonded with polymer adhesive. The governing equations employed were similar in nature to those given in [1], however, not as general. For example, only isotropic layers were considered with the stiff layers being represented by the Kirchhoff-Love theory. Furthermore, the implied edge boundary conditions are not sufficient to satisfy the principle of "layer equilibrium" [1]. The differential equations were solved by perturbation technique defining the dependent variables at three different regions along the width of the laminate. This division of the width has enabled the authors to overcome computation overflow/underflow difficulties.

Finally, Partveskii [12] has presented an approximate treatment of a free edge problem. This model combines the treatment of [13] with a model based upon a layer on an elastic foundation in order to define the distribution of interlaminar normal stress.

VARIATIONAL PRINCIPLE

The laminate considered in the present investigation is shown in Fig. 1(b). The laminate thickness comprising of $N+M$ layers is divided into two parts viz; (i) local region (l) and (ii) global region (g). N is the number of layers in the local region and M is the number of layers in the global region. In this work, we shall assume that the interface between g and l is a plane $z = \text{const.}$, although less restrictive assumptions are possible. A variational principle as described below has been used to derive the set of field equations and boundary conditions.

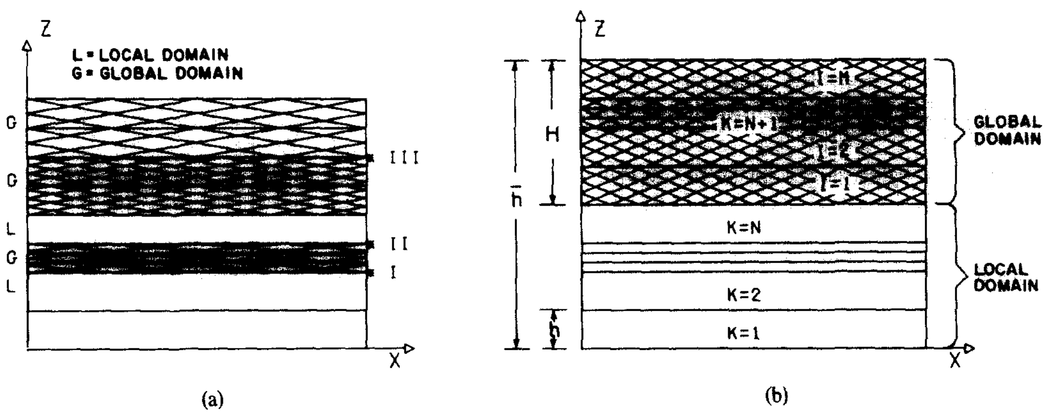

Fig. 1.(a) Laminate half thickness divided into more than one global domains with different types of interfaces. I—local-global interface, II—global-local interface, III—global-global interface. (b) Laminate half thickness with one local-global interface.

Different variational functionals in two different regions of the laminate are used such that

$$\delta\left\{\int_{V_g}\bar{w}\,\mathrm{d}v+\int_{V_l}\left[\frac{1}{2}\sigma_{ij}(u_{i,j}+u_{j,i})+w\right]\mathrm{d}v-\int_{S'}\bar{\tau}_i\,u_i\mathrm{d}s\right\}=0 \tag{1}$$

$$\text{where } \bar{w}=\bar{w}(u_i,e_{ij}),\ w=w(\sigma_{ij},e_{ij}) \tag{2}$$

and body forces are neglected. In eqn (1), the first term represents the potential energy for the global region, the second term is the Reissner variational functional for layers in the local region and the third term is the potential energy of the prescribed surface tractions. The notation used here is the same as that of Ref. [1], with the exception that the subscripts 'l' and 'g' denote respectively the local and global regions. In eqns (2), $\bar{w}$ and w are strain energy density functions, the first in terms of displacements u_i and e_{ij}, the expansional strain components, and the second in terms of stresses σ_{ij} and e_{ij}.

For a layered continuum in the local region, eqn (1) can be rewritten as

$$\delta\left\{\sum_{k=1}^{N}\int_{V_k}\left[\frac{1}{2}\sigma_{ij}(u_{i,j}+u_{j,i})-w\right]^{(k)}\mathrm{d}v_k-\int_{S'}\bar{\tau}_i\,u_i\mathrm{d}s+\int_{V_g}\bar{w}\,\mathrm{d}v\right\}=0. \tag{3}$$

where the superscript (k) attached to the bracket signifies that each variable within the bracket is associated with the kth layer. The use of Green–Gauss theorem and some mathematical manipulations in eqn (3) yield the following equation,

$$\begin{aligned}&\sum_{k=1}^{N}\int_{V_k}\left[\left(\frac{u_{i,j}+u_{j,i}}{2}-\frac{\partial w}{\partial\sigma_{ij}}\right)\delta\sigma_{ij}-\sigma_{ij,j}\,\delta u_i\right]^{(k)}\mathrm{d}v_k\\&+\int_{S'_l}(\tau_i-\bar{\tau}_i)\,\delta u_i\mathrm{d}s+\int_{S''_l}\tau_i\delta u_i\,\mathrm{d}s+\sum_{k=1}^{N-1}\int_{I''_k}(\tau_i^{(k)}\,\delta u_i^{(k)}+\tau_i^{(k+1)}\,\delta u_i^{(k+1)})\,\mathrm{d}I_k\\&-\int_{V_g}\sigma_{ij,j}\,\delta u_i\,\mathrm{d}v+\int_{S'_g}(\tau_i-\bar{\tau}_i)\,\delta u_i\,\mathrm{d}s+\int_{S''_g}\tau_i\delta u_i\,\mathrm{d}s\\&+\int_{\bar{S}}(\tau_i^{(l)}+\tau_i^{(g)})\delta u_i\,\mathrm{d}s=0\end{aligned} \tag{4}$$

where V_k is the volume of kth layer, S'_l and S''_l represent the outer surfaces bounding the local region, the former representing the portion with prescribed tractions and the latter with prescribed displacements. I''_k represents the interlaminar surface between kth and $(k+1)$th layers in local region that does not belong to S' or S'', S'_g and S''_g represent the bounding surfaces for the global domain with prescribed traction and prescribed displacement conditions, respectively. $\bar{S}$ represents the surface common to the local domain and the global domain. A superscript/subscript l denotes the local region and g denotes the global region. Clearly, as shown by eqn (4), the governing equations of elasticity can be obtained as a consequence of variational eqn (1). Equation (4) will be used to derive the field equations and boundary conditions for the two regions of the laminate.

DEVELOPMENT OF THEORY

For each layer in the local domain, the theory developed in [1] has been used. The details of the derivation of equilibrium equations and continuity and boundary conditions for this domain are not repeated in this paper. For the sake of continuity, only relevant equations are provided. Figure 2 shows the coordinate axes and thickness of a single layer in the laminate. The interlaminar stresses σ_z, τ_{xz} and τ_{yz} at the top of the layer are denoted by p_2, t_2 and s_2, respectively, while the corresponding stresses at the bottom of the layer are designated as p_1, t_1, and s_1. In the local domain the inplane stress components are assumed to vary linearly through the thickness of each ply. The substitution of these stress components in the differential equations of equilibrium [1] yields the interlaminar stress components in terms of tractions p_i, t_i,

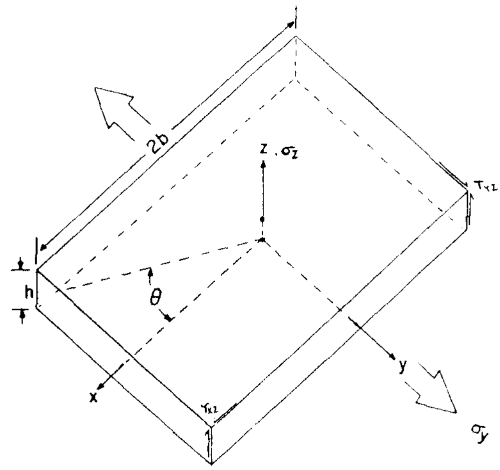

Fig. 2. Ply coordinate axes and rotation notation.

s_i ($i = 1, 2$) and force and moment resultants. These stress–stress resultant relations have been used in eqn (4) in local domain integrals. In the global domain, an assumed continuous thickness distribution of the displacement field is used. On the basis of these facts, the field equations, interfacial boundary conditions, and edge conditions within the local continuum remain the same as derived in Ref. [1]. The development of the required relations for the global domain and global/local interface follows. We assume that the global domain is composed of layers, each possessing a single plane of elastic symmetry, $z = \text{const}$. In this domain, the displacements are assumed to be of the form

$$
\begin{aligned}
u &= u^\circ(x, y) + z\Psi_x(x, y) \\
v &= v^\circ(x, y) + z\Psi_y(x, y) \\
w &= w^\circ(x, y) + z\Psi_z(x, y) + \frac{z^2}{2}\phi(x, y)
\end{aligned}
\tag{5}
$$

where u, v and w are the displacement components in the x, y and z directions, respectively. It can be seen that the number of displacement functions agrees with that given by the variational principle for each layer in the local domain. The substitution of the displacement functions (5) into the strain displacement relations of elasticity leads to the following stress–strain relations

$$
\begin{aligned}
\sigma_i &= C_{ij}(\epsilon_j^\circ + z\kappa_j - e_j) \qquad (i, j = 1, 2, 3, 6) \\
\sigma_i &= C_{ij}\left(\epsilon_j^\circ + z\kappa_j + \frac{z^2}{2}\beta_j\right) \qquad (i, j = 4, 5)
\end{aligned}
\tag{6}
$$

in standard contracted notation, where C_{ij} are the components of the anisotropic stiffness matrix, e_j are engineering expansional strain components and ϵ_i°, κ_i and β_i are defined by

$$
\begin{aligned}
&\epsilon_1^\circ = \frac{\partial u^\circ}{\partial x}, \quad \epsilon_2^\circ = \frac{\partial v^\circ}{\partial y}, \quad \epsilon_3^\circ = \psi_z \\
&\epsilon_4^\circ = \psi_y + \frac{\partial w^\circ}{\partial y}, \quad \epsilon_5^\circ = \psi_x + \frac{\partial w^\circ}{\partial x}, \quad \epsilon_6^\circ = \frac{\partial u^\circ}{\partial y} + \frac{\partial v^\circ}{\partial x} \\
&\kappa_1 = \frac{\partial \psi_x}{\partial x}, \quad \kappa_2 = \frac{\partial \psi_y}{\partial y}, \quad \kappa_3 = \phi
\end{aligned}
\tag{7}
$$

$$\kappa_4 = \frac{\partial \psi_z}{\partial y}, \quad \kappa_5 = \frac{\partial \psi_z}{\partial x}, \quad \kappa_6 = \frac{\partial \psi_x}{\partial y} + \frac{\partial \psi_y}{\partial x}$$

$$\beta_4 = \frac{\partial \phi}{\partial y}, \quad \beta_5 = \frac{\partial \phi}{\partial x}.$$

The stress components $\sigma_1, \sigma_2, \sigma_3, \sigma_4, \sigma_5, \sigma_6$ stand for $\sigma_x, \sigma_y, \sigma_z, \tau_{yz}, \tau_{xz}, \tau_{xy}$ respectively while ϵ_i° $(i = 1, 2, \ldots 6)$ represent corresponding engineering inplane strain components. We introduce the following stress and moment resultants

$$\begin{aligned} N_i &= \int_{-H/2}^{H/2} \sigma_i \, dz \\ M_i &= \int_{-H/2}^{H/2} \sigma_i z \, dz \end{aligned} \qquad (i = 1, 2, 3, 6) \tag{8}$$

where H is the thickness of the global region and N_3 and M_3 are mathematical, not physical, quantities.

Substituting eqns (6) into (8) and conducting the integration, we obtain the following constitutive relations for the global domain

$$\begin{aligned} N_\alpha &= \tilde{A}_{\alpha\beta}\epsilon_\beta^\circ + \tilde{B}_{\alpha\beta}\kappa_\beta - \bar{P}_\alpha \\ M_\alpha &= \tilde{B}_{\alpha\beta}\epsilon_\beta^\circ + D_{\alpha\beta}\kappa_\beta - \bar{Q}_\alpha \end{aligned} \qquad (\alpha, \beta = 1, 2, 3, 6)$$

$$\begin{aligned} V_i &= \tilde{A}_{ij}\epsilon_j^\circ + \tilde{B}_{ij}\kappa_j + \frac{1}{2} D_{ij}\beta_j \\ R_i &= \tilde{B}_{ij}\epsilon_j^\circ + D_{ij}\kappa_j + \frac{1}{2} F_{ij}\beta_j \\ S_i &= \frac{1}{2} D_{ij}\epsilon_j^\circ + \frac{1}{2} F_{ij}\kappa_j + \frac{1}{6} H_{ij}\beta_j \end{aligned} \qquad (i, j = 4, 5) \tag{9}$$

where

$$(\tilde{A}_{ij}, \tilde{B}_{ij}, D_{ij}, F_{ij}, H_{ij}) = \int_{-H/2}^{H/2} (1, z, z^2, z^3, z^4)\, C_{ij} \, dz \qquad (i, j = 1, 2, \ldots, 6)$$

$$\bar{P}_\alpha = \int_{-H/2}^{H/2} C_{\alpha\beta} e_\beta \, dz$$

$$\bar{Q}_\alpha = \oint_{-H/2}^{H/2} z C_{\alpha\beta} e_\beta \, dz \qquad (\alpha, \beta = 1, 2, 3, 6)$$

$$(V_i, R_i, S_i) = \int_{-H/2}^{H/2} \sigma_i (1, z, z^2) \, dz \qquad (i = 4, 5).$$

With the knowledge of the distribution of elastic properties C_{ij} and expansional strains, one can obtain the values of effective stiffness matrices $\tilde{A}$, $\tilde{B}$, D, F and H; and effective "non-mechanical" stress and moment resultants, $\bar{P}_\alpha$ and $\bar{Q}_\alpha$.

As in [1], we make the following definitions

$$(\bar{f}, f^*, \hat{f}) = \int_{-H/2}^{H/2} f\left(1, \frac{2z}{H}, \frac{4z^2}{H^2}\right) \frac{2dz}{H} \tag{10}$$

where f may represent any of the displacement variables u, v and w. Through the use of relations (5) and (10), the functions involved in the displacements for the global domain can be expressed as

$$
\begin{aligned}
u^\circ &= \frac{1}{2}\bar{u} \\
v^\circ &= \frac{1}{2}\bar{v} \\
w^\circ &= \frac{9}{8}\bar{w} - \frac{15}{8}\hat{w} \\
\psi_x &= \frac{3}{H}u^* \\
\psi_y &= \frac{3}{H}v^* \\
\psi_z &= \frac{3}{H}w^* \\
\phi &= \frac{45}{H^2}\left(\hat{w} - \frac{\bar{w}}{3}\right).
\end{aligned}
\tag{11}
$$

With these relationships, one can express the constitutive relations for the global domain in terms of the same displacement parameters as those for the local domain. This simplifies the definition of the required continuity conditions.

With the use of the assumed stress field in the local region and displacement fields in the global region in eqn (4), the required field equations, continuity and boundary conditions can be obtained. For the local region the equilibrium equations, constitutive relations, edge conditions and interfacial continuity conditions are given in [1]. For the global region the equilibrium equations, which follow from substituting (5) into (4), become

$$
\begin{aligned}
&N_{1,x} + N_{6,y} + t_2 - t_1 = 0 \\
&N_{6,x} + N_{2,y} + s_2 - s_1 = 0 \\
&-N_3 + R_{4,y} + R_{5,x} + \frac{H}{2}(p_1 + p_2) = 0 \\
&M_{1,x} + M_{6,y} - V_5 + \frac{H}{2}(t_2 + t_1) = 0 \\
&M_{6,x} + M_{2,y} - V_4 + \frac{H}{2}(s_2 + s_1) = 0 \\
&V_{5,x} + V_{4,y} + p_2 - p_1 = 0 \\
&-M_3 + S_{4,y} + S_{5,x} + \frac{H^2}{8}(p_2 - p_1) = 0
\end{aligned}
\tag{12}
$$

where the symbols t_i, s_i, and p_i $(i = 1, 2)$ retain the same meaning as defined earlier for the local domain. Assuming perfect continuity of tractions and displacements at the $g - l$ interface, the local–global interfacial conditions are given by the previous substitution into (4), as

$$t_2^{(k)} = t_1^{(k+1)}$$

$$s_2^{(k)} = s_1^{(k+1)} \tag{13}$$

$$p_2^{(k)} = p_1^{(k+1)}$$

and (a) local–global (interface I of Fig. 1a)

$$\beta_5 - S_{45}T_4 - S_{55}T_5]^{(k)} = \left[-u^\circ + \frac{H}{2}\psi_x\right]^{(k+1)}$$

$$[\beta_4 - S_{44}T_4 - S_{45}T_5]^{(k)} = \left[-v^\circ + \frac{H}{2}\psi_y\right]^{(k+1)} \tag{13a}$$

$$[\gamma_2 - S_{33}R_2]^{(k)} = \left[-w^\circ + \frac{H}{2}\psi_z - \frac{H^2}{8}\phi\right]^{(k+1)}.$$

It can be shown that if we consider more than one global region, the following interfacial conditions are required:

(b) global–local (interface II of Fig. 1a)

$$\left[u^\circ + \frac{H}{2}\psi_x\right]^{(k)} = [\alpha_5 - S_{45}Q_4 - S_{55}Q_5]^{(k+1)}$$

$$\left[v^\circ + \frac{H}{2}\psi_y\right]^{(k)} = [\alpha_4 - S_{44}Q_4 - S_{45}Q_5]^{(k+1)} \tag{13b}$$

$$\left[w^\circ + \frac{H}{2}\psi_z + \frac{H^2}{8}\phi\right]^{(k)} = [\gamma_1 - S_{33}R_1]^{(k+1)}$$

(c) global–global (interface III of Fig. 1a)

$$\left[u^\circ + \frac{H}{2}\psi_x\right]^{(k)} = \left[u^\circ - \frac{H}{2}\psi_x\right]^{(k+1)}$$

$$\left[v^\circ + \frac{H}{2}\psi_y\right]^{(k)} = \left[v^\circ - \frac{H}{2}\psi_y\right]^{(k+1)} \tag{13c}$$

$$\left[w^\circ + \frac{H}{2}\psi_z + \frac{H^2}{8}\phi\right]^{(k)} = \left[w^\circ - \frac{H}{2}\psi_z + \frac{H^2}{8}\phi\right]^{(k+1)}$$

where the parameters with superscript '$k+1$' represent those for the layer above the kth layer. The parameters on the l.h.s. of eqns (13a) and r.h.s. of eqns (13b) are defined in Ref. [1]. In the expression for R_2 of [1], the roles of p_1 and p_2 were interchanged by mistake whereas R_1 was correct. The correct expression for R_2 is

$$R_2 = \frac{(6p_2 + p_1)h^2 - 7hN_z - 30M_z}{70h}. \tag{14}$$

For the edge surface of the global domain, one term each of the following products must be prescribed:

$$N_n u_n^\circ,\ N_{ns}u_s^\circ,\ M_n\psi_n,\ M_{ns}\psi_s,\ V_n w^\circ,\ R_n\psi_z,\ S_n\phi. \tag{15}$$

The boundary conditions at the top surface are given by

$$
\begin{aligned}
t_2^{(N+1)} &= \tilde{t}_2^{(N+1)} \text{ or } u^\circ + \frac{H}{2}\psi_x = \tilde{U} \\
s_2^{(N+1)} &= \tilde{s}_2^{(N+1)} \text{ or } v^\circ + \frac{H}{2}\psi_y = \tilde{V} \qquad (16) \\
p_2^{(N+1)} &= \tilde{p}_2^{(N+1)} \text{ or } w^\circ + \frac{H}{2}\psi_z + \frac{H^2}{8}\phi = \tilde{W}
\end{aligned}
$$

where the right hand sides in the aforementioned eqns (16) represent the prescribed external tractions or displacements. The boundary conditions at the bottom surface remain the same as those explained in Ref. [1]. This completes the development of the present theory. We observe that the governing equations for the global continuum, eqns (9), (12)–(13), combined with the governing equations for the local continuum, eqns (25)–(28) of [1], and boundary conditions at the bottom and the top surfaces constitute a set of $23N + 27$ equations in terms of like number of unknowns. This system can be reduced to $13(N+1)$ equations by eliminating the force and moment resultants from the set of governing equations. Relations (15) show that 7 edge conditions are required for the global domain, while $7N$ edge conditions are required for the local domain, eqns (29) of [1].

SPECIFIC PROBLEM AND SOLUTION

The present model has been used to conduct the free edge stress analysis in a symmetric laminate consisting of $2(N+M)$ perfectly bonded layers. The laminate is subjected to forces applied only at the ends $y = \text{const.}$ such that a constant axial strain $\epsilon_y = \epsilon$ is imposed. Because of the symmetry in ply orientation of the laminate about the midplane, the deformation is symmetric with respect to x and z. Only the z symmetry will be employed in the specific problem treated, so that half of the laminate thickness has been considered. The lower N layers form the local region whereas the remaining M layers constitute the global region as shown in Fig. 1(b). The stress field in this class of problems is a function of x and z alone and consequently the force and moment resultants and the interlaminar stresses depend on x only.

LOCAL DOMAIN

By the use of strain displacement relations (1) of [14] it can be shown that the most general form of the weighted displacements within each layer is given by

$$
\begin{aligned}
\bar{u} &= U(x) - \frac{C_1 y^2}{2} + C_3 y \\
\bar{v} &= V(x) + C_1 xy + C_2 y \\
h\bar{w} &= W(x) - 6C_5 xy + 3C_4 y - 3C_6 y^2 \\
u^* &= \psi(x) + C_5 y \qquad (17) \\
v^* &= \Omega(x) + C_6 y \\
w^* &= \phi(x) \\
h\hat{w} &= \chi(x) - 2C_5 xy + C_4 y - C_6 y^2
\end{aligned}
$$

where $U, V, \ldots \chi$ are arbitrary functions of x and $C_1, C_2, \ldots, C_6$ are constants. We should recall that the stress strain relations (3) of [14] must be written for each layer. The use of the foregoing relations in the strain-displacement relations yields

$$
\begin{aligned}
\epsilon_1 &= \frac{h}{2}\bar{u}_{,x} = \frac{h}{2}U'(x)\\
\epsilon_2 &= \frac{h}{2}\bar{v}_{,y} = \frac{h}{2}(C_1x + C_2)\\
\epsilon_3 &= 3w^* = 3\phi(x)\\
\epsilon_6 &= \frac{h}{2}(\bar{u}_{,y} + \bar{v}_{,x}) = \frac{h}{2}[V'(x) + C_3]\\
\kappa_1 &= \frac{h^2}{4}u^*_{,x} = \frac{h^2}{4}\psi'(x)\\
\kappa_2 &= \frac{h^2}{4}v^*_{,y} = \frac{h^2}{4}C_6\\
\kappa_3 &= \frac{5}{4}h(3\hat{w} - \bar{w}) = \frac{5}{4}[3\chi(x) - W(x)]\\
\kappa_6 &= \frac{h^2}{4}(u^*_{,y} + v^*_{,x}) = \frac{h^2}{4}[\Omega'(x) + C_5]\\
\epsilon_4 &= \frac{5h}{8}(\bar{w}_{,y} - \hat{w}_{,y}) + \frac{5v^*}{2} = \frac{5}{4}[2\Omega(x) - 2C_5x + C_4]\\
\epsilon_5 &= \frac{5h}{8}(\bar{w}_{,x} - \hat{w}_{,x}) + \frac{5u^*}{2} = \frac{5}{8}[W'(x) - \chi'(x) + 4\psi(x)]
\end{aligned}
\tag{18}
$$

in each layer, where h is the layer thickness. The substitution of the strain components (18) in the equilibrium equations (28) of [1], through the constitutive relations (25), [1], gives

$$A_{11}\frac{h}{2}U'' + 3A_{13}\phi' + A_{16}\frac{h}{2}V'' + A_{13}\frac{S_{33}h}{10}(P_{1,x} + p_{2,x}) + t_2 - t_1 = A_{1j}e_{j,x} - \frac{A_{12}}{2}hc_1$$

$$A_{16}\frac{h}{2}U'' + 3A_{36}\phi' + A_{66}\frac{h}{2}V'' + \frac{A_{36}S_{33}h}{10}(p_{1,x} + p_{2,x}) + s_2 - s_1 = A_{6j}e_{j,x} - \frac{A_{26}}{2}hc_1$$

$$A_{13}\frac{h}{2}U' + 3A_{33}\phi + A_{36}\frac{h}{2}V' + \frac{h}{10}(A_{33}S_{33} - 5)(p_1 + p_2) + \frac{h^2}{12}(t_{1,x} - t_{2,x})$$

$$= A_{3j}e_j - A_{23}\frac{h}{2}(C_1X + C_2) - A_{36}\frac{h}{2}C_3$$

$$\frac{B_{11}h^2}{4}\psi'' + \frac{5}{4}B_{13}[3\chi' - W'] + \frac{B_{16}h^2}{4}\Omega'' + \frac{B_{13}S_{33}h^2}{28}(p_{2,x} - p_{1,x}) - \frac{5}{2}A_{45}\Omega$$

$$-\frac{5}{8}A_{55}(W' - \chi' + 4\psi) + \frac{5h}{12}(t_1 + t_2) = \frac{5}{4}A_{45}(C_4 - 2C_5x)$$

$$\frac{B_{16}h^2}{4}\psi'' + \frac{5}{4}B_{36}(3\chi' - W') + \frac{B_{66}h^2}{4}\Omega'' + \frac{B_{36}S_{33}h^2}{28}(p_{2,x} - p_{1,x}) - \frac{5}{2}A_{44}\Omega$$

$$-\frac{5}{8}A_{45}(W' - \chi' + 4\psi) + \frac{5h}{12}(s_1 + s_2) = \frac{5}{4}A_{44}(C_4 - 2C_5X)$$

$$\frac{5}{2}A_{45}\Omega'+\frac{5}{8}A_{55}(W''-\chi''+4\psi')+\frac{h}{12}(t_{1,x}+t_{2,x})+p_2-p_1=\frac{5}{2}A_{45}C_5$$

$$\frac{5}{2}B_{13}\psi'+\frac{25}{2}\frac{B_{33}}{h^2}(3\chi-W)+\frac{5}{2}B_{36}\Omega'+\frac{1}{14}(5B_{33}S_{33}-14)(p_2-p_1)-\frac{h}{12}(t_{1,x}+t_{2,x})$$

$$=-\frac{5}{2}B_{23}C_6-\frac{5}{2}B_{36}C_5. \tag{19}$$

These equations are valid within each layer. Similarly the remaining field equations, the interface continuity conditions, are given by

$$\left\{\frac{5}{8}\chi'-\frac{1}{8}W'-\frac{h}{2}\phi'+U-\frac{5}{2}\psi-\frac{h}{12}[S_{55}(3t_1-t_2)+S_{45}(3s_1-s_2)]\right\}^{(k+1)}$$

$$+\left\{\frac{5}{8}\chi'-\frac{1}{8}W'+\frac{h}{2}\phi'-U-\frac{5}{2}\psi-\frac{h}{12}[S_{55}(3t_2-t_1)+S_{45}(3s_2-s_1)]\right\}^{(k)}$$

$$=3(C_5^{(k+1)}+C_5^{(k)})y+(C_3^{(k)}-C_3^{(k+1)})y+\frac{1}{2}(C_1^{(k+1)}-C_1^{(k)})y^2.$$

$$\left\{V-\frac{5}{2}\Omega-\frac{h}{12}[S_{45}(3t_1-t_2)+S_{44}(3s_1-s_2)]\right\}^{(k+1)}$$

$$+\left\{-V-\frac{5}{2}\Omega-\frac{h}{12}[S_{45}(3t_2-t_1)+S_{44}(3s_2-s_1)]\right\}^{(k)}$$

$$=\frac{1}{2}(C_5^{(k+1)}+C_5^{(k)})x-\frac{1}{4}(C_4^{(k)}+C_4^{(k+1)})+3(C_6^{(k+1)}+C_6^{(k)})y$$

$$+(C_1^{(k)}-C_1^{(k+1)})xy+(C_2^{(k)}-C_2^{(k+1)})y.$$

$$\left\{-\frac{S_{33}}{35}\left[-\frac{7A_{13}h}{2}U'+\left(-21A_{33}+\frac{105}{S_{33}}\right)\phi-\frac{7A_{36}h}{2}V'+\frac{15}{2}B_{13}h\psi'\right.\right.$$

$$+\left(\frac{225B_{33}}{2h}-\frac{525}{2S_{33}h}\right)\chi+\left(-\frac{75}{2h}B_{33}+\frac{105}{2S_{33}h}\right)W+\frac{15B_{36}h}{2}\Omega'$$

$$\left.\left.+hp_1\left(6-7\frac{A_{33}}{10}S_{33}-\frac{15B_{33}S_{33}}{14}\right)+hp_2\left(1-\frac{7A_{33}}{10}S_{33}+\frac{15B_{33}}{14}S_{33}\right)\right]\right\}^{(k+1)}$$

$$+\left\{-\frac{S_{33}}{35}\left[-\frac{7A_{13}h}{2}U'+\left(-21A_{33}+\frac{105}{S_{33}}\right)\phi-\frac{7A_{36}h}{2}V'-\frac{15}{2}B_{13}h\psi'\right.\right.$$

$$+\left(-\frac{225B_{33}}{2h}+\frac{525}{2S_{33}h}\right)\chi+\left(\frac{75}{2h}B_{33}-\frac{105}{2S_{33}h}\right)W-\frac{15B_{36}h}{2}\Omega'$$

$$\left.\left.+hp_1\left(1-\frac{7A_{33}S_{33}}{10}+\frac{15B_{33}S_{33}}{14}\right)+hp_2\left(6-\frac{7A_{33}S_{33}}{10}-15\frac{B_{33}}{14}S_{33}\right)\right]\right\}^{(k)}$$

$$=6\left(\frac{C_5^{(k+1)}}{h_{k+1}}-\frac{C_5^{(k)}}{h_k}\right)xy+3\left(\frac{C_4^{(k)}}{h_k}-\frac{C_4^{(k+1)}}{h_{k+1}}\right)y+3\left(\frac{C_6^{(k+1)}}{h_{k+1}}+\frac{C_6^{(k)}}{h_k}\right)y^2$$

$$-\frac{x}{10}(S_{33}^{(k+1)}A_{23}^{(k+1)}h_{k+1}C_1^{(k+1)}+S_{33}^{(k)}A_{23}^{(k)}h_kC_1^{(k)})+\frac{1}{35}\left\{S_{33}\left[-7\frac{A_{23}h}{2}C_2-7\frac{A_{36}h}{2}C_3+7A_{3j}e_j\right.\right.$$

$$\left.\left.+\frac{15}{2}B_{23}hC_6+\frac{15}{2}B_{36}hC_5\right]\right\}^{(k+1)}+\frac{1}{35}\left\{S_{33}\left[-7\frac{A_{23}}{2}hC_2-7\frac{A_{36}}{2}hC_3+7A_{3j}e_j\right.\right.$$

$$\left.\left.-\frac{15B_{23}h}{2}C_6-\frac{15B_{36}h}{2}C_5\right]\right\}^{(k)}$$

$$t_2^{(k)} = t_1^{(k+1)}$$

$$s_2^{(k)} = s_1^{(k+1)} \tag{20}$$

$$p_2^{(k)} = p_1^{(k+1)}.$$

The last six equations are valid for $k = 1, 2, --, N-1$, since we recall that N is the number of layers in the local region. Due to the symmetric lamination geometry, the interlaminar shear stress components and the transverse displacement component W all vanish on the central plane, $z = 0$. We shall take advantage of these conditions by considering only the upper half of the laminate, i.e. $z > 0$. Thus, the boundary conditions at the lower surface reduce to

$$\frac{S_{33}^{(1)}}{35}\left[-\frac{7A_{13}}{2}hU' + \left(-21A_{33} + \frac{105}{S_{33}}\right)\phi - \frac{7A_{36}}{2}hV' + \frac{15}{2}B_{13}h\psi'\right.$$

$$+\left(\frac{225B_{33}}{2h} - \frac{35}{2S_{33}}\frac{15}{h}\right)\chi + \left(-\frac{75}{2h}B_{33} + \frac{105}{2hS_{33}}\right)W$$

$$\left.+\frac{15B_{36}}{2}h\Omega' + hp_1\left(6 - 7\frac{A_{33}S_{33}}{10} - \frac{15B_{33}S_{33}}{14}\right) + hp_2\left(1 - \frac{7A_{33}}{10}S_{33} + \frac{15B_{33}}{14}S_{33}\right)\right]^{(1)}$$

$$= \left\{-\frac{6C_5}{h}xy + \frac{3C_4}{h}y - \frac{3C_6}{h}y^2 + \frac{x}{10}S_{33}A_{23}hC_1 - \frac{S_{33}}{35}\left[-\frac{7A_{23}}{2}hC_2 - \frac{7A_{36}}{2}hC_3 + 7A_{3j}e_j\right.\right.$$

$$\left.\left.+\frac{15}{2}B_{23}hC_6 + \frac{15}{2}B_{36}hC_5\right]\right\}^{(1)}$$

and

$$t_1^{(1)} = s_1^{(1)} = 0. \tag{21}$$

Since eqns (19)–(21) must be satisfied for all values of y, it follows that

$$C_4^{(k)} = C_5^{(k)} = C_6^{(k)} = 0, \qquad k = 1, 2, \ldots N$$

and

$$C_1^{(k+1)} = C_1^{(k)},\ C_2^{(k+1)} = C_2^{(k)},\ C_3^{(k+1)} = C_3^{(k)}, \qquad k = 1, 2, \ldots N-1$$

so that C_1, C_2 and C_3 are the same for each layer. Further, it has been shown in [14] that

$$C_1 = C_3 = 0$$

$$C_2 = 2\epsilon.$$

We will use these values of C_i in the forthcoming work.

GLOBAL DOMAIN

With the aid of relationships (11), we can obtain the following strain displacement relations for the global domain

$$\epsilon_x^\circ = \frac{1}{2}\bar{u}_{,x}$$

$$\epsilon_y^\circ = \frac{1}{2}\bar{v}_{,y}$$

$$\epsilon_z^\circ = \frac{3}{H} w^*$$

$$\epsilon^\circ_{xy} = \frac{1}{2}(\bar{u},_y + \bar{v},_x)$$

$$\epsilon_{yz}^\circ = \frac{3}{H} v^* + \frac{9}{8}\bar{w},_y - \frac{15}{8}\hat{w},_y$$

$$\epsilon_{xz}^\circ = \frac{3}{H} u^* + \frac{9}{8}\bar{w},_x - \frac{15}{8}\hat{w},_x$$

$$\kappa_1 = \frac{3}{H} u^*,_x$$

$$\kappa_2 = \frac{3}{H} v^*,_y \tag{22}$$

$$\beta_4 = \frac{45}{H^2}(\hat{w},_y - \frac{1}{3}\bar{w},_y)$$

$$\kappa_3 = \frac{45}{H^2}\left(\hat{w} - \frac{\bar{w}}{3}\right)$$

$$\beta_5 = \frac{45}{H^2}\left(\hat{w},_x - \frac{1}{3}\bar{w},_x\right)$$

$$\kappa_4 = \frac{3}{H} w^*,_y$$

$$\kappa_5 = \frac{3}{H} w^*,_x$$

$$\kappa_6 = \frac{3}{H}(u^*,_y + v^*,_x)$$

where $\bar{u}$, u^*,---$\hat{w}$ now refer to the global domain. We may also observe that the relations (17) are also valid for the global domain. The substitution of the values of inplane strains and curvatures in the stress–strain relations (9) through eqns (17) and their subsequent use in eqns (12) yield the following form of equilibrium equations

$$\frac{1}{2}\tilde{A}_{11}U'' + \frac{3}{H}\tilde{A}_{13}\phi' + \frac{1}{2}\tilde{A}_{16}V'' + \frac{3}{H}\tilde{B}_{11}\psi'' + \frac{3}{H}\tilde{B}_{16}\Omega''$$

$$+ \frac{45}{H^3}\tilde{B}_{13}\left(\chi' - \frac{1}{3}W'\right) + t_2 - t_1 - \bar{P}_{1,x} = 0$$

$$\frac{1}{2}\tilde{A}_{61}U'' + \frac{3}{H}\tilde{A}_{63}\phi' + \frac{1}{2}\tilde{A}_{66}V'' + \frac{3}{H}\tilde{B}_{61}\psi'' + \frac{3}{H}\tilde{B}_{66}\Omega''$$

$$+ \frac{45}{H^3}\tilde{B}_{63}\left(\chi' - \frac{1}{3}W'\right) + s_2 - s_1 - P_{6,x} = 0$$

$$\frac{1}{2}\tilde{A}_{31}U' - \frac{3}{H}D_{55}\phi'' + \frac{3}{H}\tilde{A}_{33}\phi + \frac{1}{2}\tilde{A}_{36}V' + \frac{3}{H}(\tilde{B}_{31} - \tilde{B}_{55})\psi'$$

$$+ \frac{3}{H}(\tilde{B}_{36} - \tilde{B}_{45})\Omega' + \left(\frac{15}{8H}\tilde{B}_{55} - \frac{45}{2H^3}F_{55}\right)\chi'' + \frac{45}{H^3}\tilde{B}_{33}\chi$$

$$+ \left(\frac{15}{2H^3}F_{55} - \frac{9}{8H}\tilde{B}_{55}\right)W'' - \frac{15}{H^3}\tilde{B}_{33}W + \tilde{A}_{32}\epsilon - \bar{p}_3 - \frac{H}{2}(p_1 + p_2) = 0$$

$$\frac{1}{2}\tilde{B}_{11}U''+\frac{3}{H}(\tilde{B}_{13}-\tilde{B}_{55})\phi'+\frac{1}{2}\tilde{B}_{16}V''+\frac{3}{H}D_{11}\psi''-\frac{3}{H}\tilde{A}_{55}\psi$$

$$+\frac{3}{H}D_{16}\Omega''-\frac{3}{H}\tilde{A}_{45}\Omega+\left(\frac{45}{H^3}D_{13}+\frac{15}{8H}\tilde{A}_{55}-\frac{45}{2H^3}D_{55}\right)\chi'$$

$$-\left(\frac{15}{H^3}D_{13}+\frac{9}{8H}\tilde{A}_{55}-\frac{15D_{55}}{2H^3}\right)W'+\frac{H}{2}(t_2+t_1)-\bar{Q}_{1,x}=0$$

$$\frac{1}{2}B_{61}U''+\frac{3}{H}(\tilde{B}_{63}-\tilde{B}_{45})\phi'+\frac{1}{2}\tilde{B}_{66}V''+\frac{3}{H}D_{61}\psi''-\frac{3}{H}\tilde{A}_{45}\psi$$

$$+\frac{3}{H}D_{66}\Omega''-\frac{3}{H}\tilde{A}_{44}\Omega+\left(\frac{45}{H^3}D_{63}+\frac{15}{8H}\tilde{A}_{45}-\frac{45D_{45}}{2H^3}\right)\chi'$$

$$-\left(\frac{15}{H^3}D_{63}+\frac{9}{8H}\tilde{A}_{45}-\frac{15}{2H^3}D_{45}\right)W'+\frac{H}{2}(s_1+s_2)-\bar{Q}_{6,x}=0$$

$$\frac{3}{H}\tilde{B}_{55}\phi''+\frac{3}{H}\tilde{A}_{55}\psi'+\frac{3}{H}\tilde{A}_{45}\Omega'+\left(\frac{45}{2H^3}D_{55}-\frac{15}{8H}\tilde{A}_{55}\right)\chi''$$

$$+\left(\frac{9}{8H}\tilde{A}_{55}-\frac{15}{2H^3}D_{55}\right)W''+p_2-p_1=0$$

$$\frac{1}{2}\tilde{B}_{31}U'-\frac{3}{2H^2}F_{55}\phi''+\frac{3}{H}\tilde{B}_{33}\phi+\frac{1}{2}\tilde{B}_{36}V'+\frac{3}{H}\left(D_{31}-\frac{D_{55}}{2}\right)\psi' \tag{23}$$

$$+\frac{3}{H}\left[D_{36}-\frac{D_{45}}{2}\right)\Omega'+\left(\frac{15}{16H}D_{55}-\frac{45}{4H^3}H_{55}\right)\chi''+\frac{45}{H^3}D_{33}\chi$$

$$+\left(\frac{15}{4H^3}H_{55}-\frac{9}{16H}D_{55}\right)W''-\frac{15}{H^3}D_{33}W+B_{32}\epsilon-\bar{Q}_3-\frac{H^2}{2}(p_2-p_1)=0.$$

As for the local domain, in the foregoing equations we have used

$$C_1=C_3=C_4=C_5=C_6=0$$

$$C_2=2\epsilon.$$

In eqn (23) the effective modulus matrices defined in eqns (9) are used. The continuity conditions (13) and (13a) at local–global interface, on substitutions of (17) and (14) of the present paper and eqns (16) of [1], reduce to

$$t_2^{(N)}=t_1^{(N+1)}$$

$$s_2^{(N)}=s_1^{(N+1)}$$

$$p_2^{(N)}=p_1^{(N+1)}$$

$$\left\{\frac{5}{8}\chi'-\frac{1}{8}W'+\frac{h}{2}\phi'-U-\frac{5}{2}\psi-\frac{h}{12}[S_{55}(3t_2-t_1)+S_{45}(3s_2-s_1)]\right\}^{(N)}=(-U+3\psi)^{(N+1)}$$

$$\left\{-V-\frac{5}{2}\Omega-\frac{h}{12}[S_{45}(3t_2-t_1)+S_{44}(3s_2-s_1)]\right\}^{(N)}=(-V+3\Omega)^{(N+1)}$$

$$\left\{\frac{S_{33}}{35}\left[\frac{7A_{13}}{2}hU'+\left(-21A_{33}+\frac{105}{S_{33}}\right)\phi-\frac{7}{2}A_{36}hV'-\frac{15}{2}hB_{13}\psi'\right.\right.$$

$$+\left(-\frac{225}{2h}B_{33}+\frac{525}{2hS_{33}}\right)\chi+\left(\frac{75}{2h}B_{33}-\frac{105}{2hS_{33}}\right)W-\frac{15h}{2}B_{36}\Omega'$$

$$\left.\left.+hp_1\left(1-\frac{7A_{33}}{10}S_{33}+\frac{15B_{33}S_{33}}{14}\right)+hp_2\left(6-\frac{7A_{33}S_{33}}{10}-\frac{15B_{33}S_{33}}{14}\right)\right]\right\}^{(N)}$$

$$=\left\{\frac{15}{2H}\chi-3\phi-\frac{3}{2H}W\right\}^{(N+1)}. \tag{25}$$

The boundary conditions at the top surface considered in the present investigation are:

$$s_2^{(N+1)}=t_2^{(N+1)}=p_2^{(N+1)}=0. \tag{26}$$

EDGE BOUNDARY CONDITIONS

We now turn our attention to the edge boundary conditions, which require consideration of N_x, N_{xy}, V_x, M_x, M_{xy}, t_1 and t_2 for each layer on $x = \pm b$, since no displacement edge conditions are involved in the present class of boundary value problems. However, all these functions cannot be independently prescribed because of the consequences of interface continuity and overall equilibrium of the entire laminate. That is, the interface continuity conditions given by the fourth of (20) prohibit arbitrarily prescribed values of $t_1^{(k)}$ and $t_2^{(k)}$. Furthermore, $t_1^{(1)}$ and $t_2^{(N+1)}$ have already been specified by (21) and (26) for all values of x. These relations, in conjunction with the first equilibrium equation, see (26) of [1], and eqn (12), can be used to establish the result

$$\sum_{k=1}^{N+1} N_{x,x}^{(k)}=0 \tag{27}$$

which requires that

$$\sum_{k=1}^{N+1} N_x^{(k)}(b)-\sum_{k=1}^{N+1} N_x^{(k)}(-b)=0. \tag{28}$$

Therefore, only $2N+1$ values of $N_x^{(k)}$ can be arbitrarily prescribed on the edges $x = \pm b$. We can make the same statement regarding $N_{xy}^{(k)}$ since an equation of the form (28) can be derived in similar fashion for this function. Hence, the edge boundary conditions for the local domain may be expressed as

$$N_x^{(k)}(\pm b)=N_{xy}^{(k)}(\pm b)=V_x^{(k)}(\pm b)=M_x^{(k)}(\pm b)=M_{xy}^{(k)}(\pm b)=0$$

$$t_2^{(k)}(\pm b)=0 \quad (k=1,2,\ldots N) \tag{29}$$

while those for the global domain are

$$N_x^{(N+1)}(b)=N_{xy}^{(N+1)}(b)=V_x^{(N+1)}(\pm b)=M_x^{(N+1)}(\pm b)$$

$$=M_{xy}^{(N+1)}(\pm b)=R_x^{(N+1)}(\pm b)=S_x^{(N+1)}(\pm b)=0. \tag{30}$$

Thus, the present boundary value problem consists of the differential equations (19), (20), (23) and (25) subject to boundary conditions (21), (26), (29) and (30).

The general solution for each dependent variable consists of the sum of two parts: (i) a complementary solution defined by the homogeneous form of (19), (20), (23) and (25), and (ii) a particular solution. In the particular solution (denoted by subscript P), the only nonvanishing functions are given by

$$\phi_P^{(k)} = a_1^{(k)}, \quad \chi_P^{(k)} = a_2^{(k)} + a_0, \quad W_P^{(k)} = 3a_2^{(k)}, \quad k = 1, 2, \ldots, N+1 \tag{31}$$

where $a_i^{(k)}$ $(i = 1, 2)$ are constants given by substituting (31) into (15) and (20) to get

$$a_1^{(k)} = \frac{1}{3A_{33}^{(k)}}(A_{3\beta}^{(k)}\bar{a}_\beta^{(k)} - A_{23}^{(k)}h_k\epsilon), a_0 = 0, \quad k = 1, 2, \ldots, N$$

$$a_2^{(1)} = h_1^{(1)}a_1$$

$$\frac{a_2^{(k+1)}}{h_{k+1}} = a_1^{(k+1)} + a_1^{(k)} + \frac{a_2^{(k)}}{h_k}, \quad k = 1, 2, \ldots, N-1 \tag{32}$$

where $\bar{a}_\beta = he_\beta$ $(\beta = 1, 2, 3, 6)$. Similarly using (31) in (23) and (25), we get

$$a_1^{(N+1)} = \frac{1}{\tilde{A}_{33}^{(N+1)}}\left[\frac{H}{3}(\bar{P}_3 - \epsilon\tilde{A}_{23}) - \frac{15}{H^2}a_0\tilde{B}_{33}\right]^{(N+1)}$$

$$a_0 = \frac{H^3}{45}\left[\left\{\tilde{B}_{33}(\bar{P}_3 - \epsilon\tilde{A}_{23}) - \tilde{A}_{33}(\bar{Q}_3 - \epsilon\tilde{B}_{23})\right\}/(\tilde{B}_{33}^2 - \tilde{A}_{33}D_{33})\right]^{(N+1)}$$

$$a_2^{(N+1)} = -\frac{5}{2}a_0 + H\left(a_1^{(N)} + \frac{a_2^{(N)}}{h_N} + a_1^{(N+1)}\right). \tag{33}$$

Since the field equations are linear differential equations with constant coefficients, the complementary solution (subscript H) for each dependent variable consists of a series of terms of the form

$$f_H^{(k)} = F^{(k)}e^{\lambda x} \quad k = 1, 2, \ldots, N+1 \tag{34}$$

where $f^{(k)}$ represents any of the dependent variables and $F^{(k)}$ are constants. The substitution of (34) in the homogeneous form of eqns (19), (20), (23) and (25) yields a system of $13(N+1)$ linear algebraic equations. This set of equations can be written in the following matrix form

$$[\mathbf{J}][\mathbf{F}] = 0 \tag{34a}$$

where $\mathbf{J}$ is a $13(N+1) \times 13(N+1)$ matrix dependent upon material properties of the laminate and λ, and $\mathbf{F}$ is a vector of constants $F^{(k)}$ defined in (34). For a nontrivial solution of eqn (34a), the determinant of the coefficient matrix $\mathbf{J}$ has been equated to zero and the resulting equation has been solved for specific values of λ by the method of Jenkins and Traub [15].

The algebraic expressions for the elements of $\mathbf{J}$ were not written owing to the complexity of such expressions, even in the simplest cases. The computer-calculated values of λ have been used to carry out the required analysis. The extreme (highest and the lowest)powers of λ in the polynomial expansion of $[\mathbf{J}]$ were investigated for small values of $N+1$ and deduced for arbitrary values of N and M. It was found during numerical calculations that for incompatible extreme powers of λ, the solutions for λ were nonconvergent in the iterative procedure, whereas for compatible powers these converged very rapidly. Following the procedure described in [1], the following observations were made (i) only even powers of λ occur in the determinant, (ii) the lowest power of λ is λ^4, and (iii) the highest power of λ is $\lambda^{12(N+1)}$.

As in [1], the functions corresponding to the repeated zero roots for λ can be written in the following form:

$$U_{H0}^{(k)} = A_1x + A_0$$

$$V_{H0}^{(k)} = C_1x + C_0$$

$$\begin{aligned} \phi_{H0}^{(k)} &= B_0^{(k)} \\ \chi_{H0}^{(k)} &= E_0^{(k)} \\ W_{H0}^{(k)} &= 3(E_0^{(k)} + d_0) \\ d_0 &= 0 \text{ for } k = 1, 2, \ldots, N \end{aligned} \tag{35}$$

where

$$\begin{aligned} B_0^{(k)} &= -\frac{(A_{13}^{(k)} A_1 + A_{36}^{(k)} C_1) h_k}{6 A_{33}^{(k)}}, \quad k = 1, 2, \ldots, N \\ E_0^{(1)} &= h_1 B_0^{(1)} \\ \frac{E_0^{(k+1)}}{h_{k+1}} &= B_0^{(k)} + \frac{E_0^{(k)}}{h_k} + B_0^{(k+1)}, \quad k = 1, 2, \ldots, N-1 \\ B_0^{(N+1)} &= \frac{-H}{6(A_{33} D_{33} - \tilde{B}_{33}^2)} \{(\tilde{A}_{13} D_{33} - \tilde{B}_{13} \tilde{B}_{33}) A_1 + (\tilde{A}_{36} D_{33} - \tilde{B}_{36} \tilde{B}_{33}) C_1\} \\ d_0 &= \frac{H^2}{15 D_{33}} \left\{ \tilde{B}_{33} B_0^{(N+1)} + \frac{H}{6} (\tilde{B}_{13} A_1 + \tilde{B}_{36} C_1) \right\} \\ E_0^{(N+1)} &= H \left(B_0^{(N)} + \frac{E_0^{(N)}}{h_N} + B_0^{(N+1)} \right) + \frac{3}{2} d_0. \end{aligned} \tag{36}$$

The constants A_0 and C_0 define rigid body translation of the laminate as a unit. The remaining constants in (35) can all be expressed in terms of A_1 and C_1. Hence, two constants which effect the stress distribution have been introduced in the repeated zero part of the homogeneous solutions.

The remaining portion of the complementary solution consists of functions of the form (34) corresponding to the $12(N+1)-2$ nonzero values of λ (we are assuming that these roots are all distinct). In the present formulation the number of nonzero values of λ is higher than that obtained in [1]. This is due to the difference in equilibium equations for the global domain. The requisite number of extra boundary conditions are obtained from the last two terms of (15). These roots occur in pairs of complex conjugates $a \pm ib$. Using the eigenvalues and eigenvectors and the edge conditions (29) and (30) we can obtain the solution for the $13(N+1)$ functions appearing in (19), (20), (23) and (25) as

$$f^{(k)} = \sum_{m=1}^{12(N+1)-4} F_m^{(k)} e^{\lambda m x} + f_{H0}^{(k)} + f_p^{(k)}, \quad (k = 1, 2, N+1) \tag{37}$$

where the last two terms are defined by eqns (31)–(33), (35) and (36). The force and moment resultants can be computed by substituting the results of (37) into (17) and (18) and thence into the constitutive relations.

When each layer is isotropic and/or oriented at an angle of 0 or 90°, the compliance components S_{16}, S_{26}, S_{36} and S_{45} and expansional strain e_6 vanish in each layer. This leads to the vanishing of $U^{(k)}$, $\phi^{(k)}$, $t_1^{(k)}$, $t_2^{(k)}$, $N_{xy}^{(k)}$ and $M_{xy}^{(k)}$. Consequently, the number of field equations and boundary conditions is reduced. This case must be treated separately by specializing the present derivation as in [1].

In the model presented in [1], laminates consisting of a moderate number of layers ($N > 6$) could not be analyzed because of computer overflow/underflow limitations. Furthermore, while the present work has focused on a fairly special case (only one global-local interface), more general arrangements of global and local domains can be treated by simple modifications of the general relations given here, e.g. eqns (13a–c) must reflect the proper positions of global and local media. In this way arbitrary layers can be modeled in a local fashion to define the stress field in the entire body, if desired.

RESULTS AND DISCUSSION

For the computation of numerical results, T300/5208 graphite epoxy material, with the following elastic properties, has been considered:

$$E_{11} = 20 \times 10^6 \text{ psi}, E_{22} = E_{33} = 1.4 \times 10^6 \text{ psi}$$

$$G_{12} = G_{13} = 0.8 \times 10^6 \text{ psi}, G_{23} = 0.6 \times 10^6 \text{ psi}$$

$$\nu_{12} = \nu_{13} = 0.3, \nu_{23} = 0.6$$

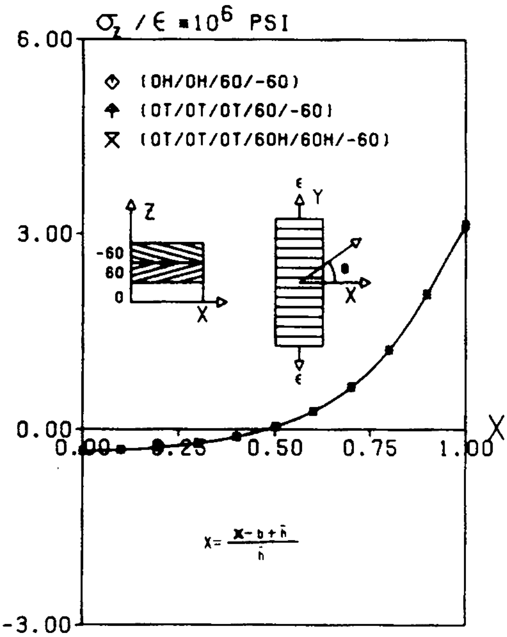

Fig. 3. Stress distribution $\sigma_z/(\epsilon \times 10^6)$ psi vs width coordinate X at the mid surface of the laminate.

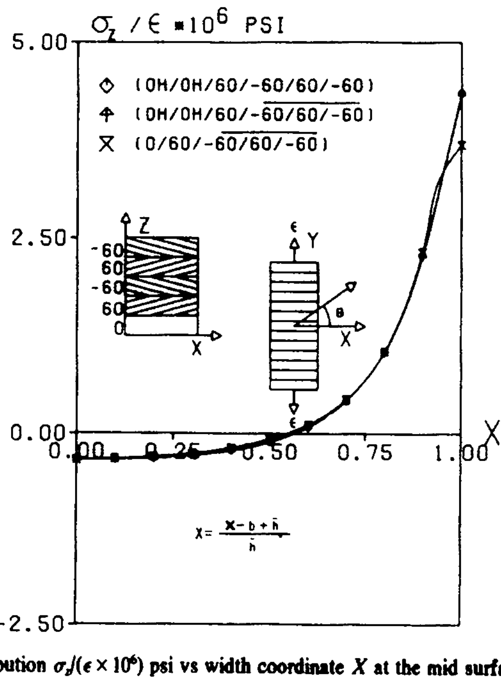

Fig. 4. Stress distribution $\sigma_z/(\epsilon \times 10^6)$ psi vs width coordinate X at the mid surface of the laminate.

where E, G and ν stand for Young's modulus, shear modulus and Poisson's ratio, respectively. The subscripts denote the corresponding directions, where 1, 2, 3 stand for x, y, z, respectively, and ν_{ij} is the Poisson ratio measuring strain in the j direction caused by uniaxial stress σ_i.

In most of the earlier investigations on edge effects, the Poisson ratios ν_{12}, ν_{13} and ν_{23} were taken to be equal. A recent experimental study has revealed the values shown above. In particular, the magnitude of ν_{23} was found to be equal to approx. 0.6 [16].

Figures 3–10 depict the distribution of stress components σ_z, τ_{xz} and τ_{yz} along the width for various laminates. The abscissa is the laminate width coordinate normalized by the half laminate thickness, such that in these diagrams $X = 1$ represents the free edge of the laminate and $X = 0$ represents a point at a distance equal to the half laminate thickness from the edge.

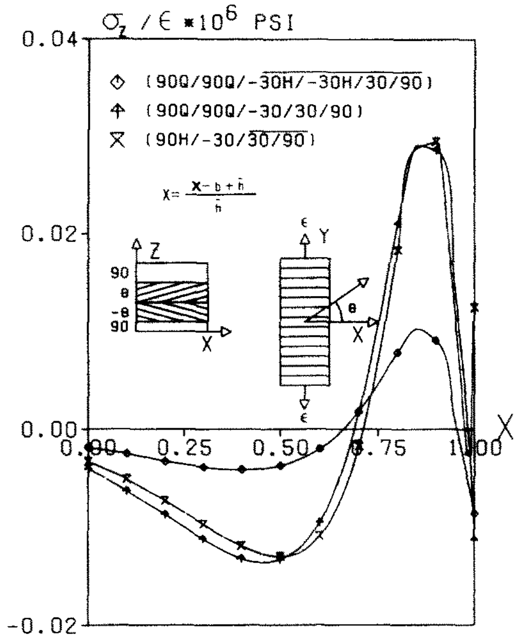

Fig. 5. Stress distribution $\sigma_z/(\epsilon \times 10^6)$ psi vs width coordinate X at the mid surface of the laminate.

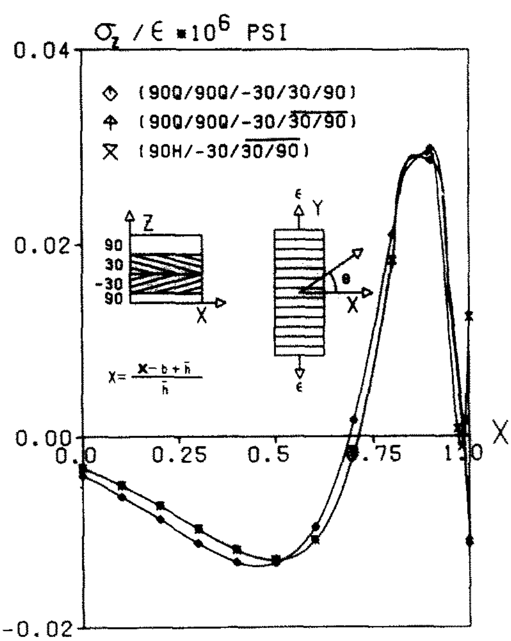

Fig. 6. Stress distribution $\sigma_z/(\epsilon \times 10^6)$ psi vs width coordinate X at the mid surface of the laminate.

These results correspond to the limiting response as the laminate width approaches infinity and can be shown to be very accurate for laminates in which the width is more than (approx.) twice the total thickness. The coordinate axes, stacking sequence and loading conditions are shown in the figures. In the symbolic notation for laminate ply orientations, a numeral followed by H, Q and T denote one half, one quarter or one third, respectively, thickness of the corresponding layer. The layers under a bar constitute the global region.

Figure 3 shows the stress component σ_z at the laminate mid surface versus X for a $(0/\pm60)_s$-laminate, calculated by using the formulation of [1], for three different layer thickness representations. The first representation is such that the first layer from the midsurface (0°) is modeled as two sublayers, each of half the layer thickness $h/2$, and the other two layers are

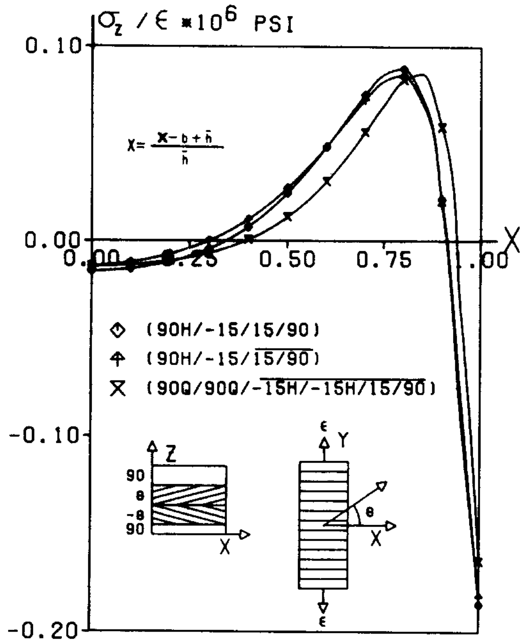

Fig. 7. Stress distirbution $\sigma_z/(\epsilon\times10^6)$ psi vs width coordinate X at the mid surface of the laminate.

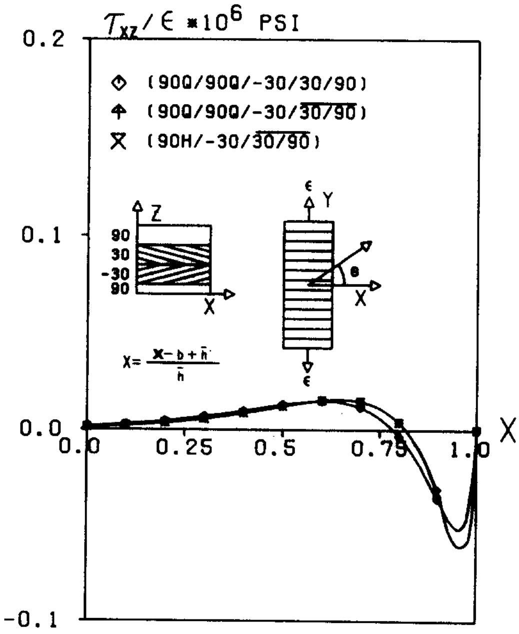

Fig. 8. Stress distribution $\tau_{xz}/(\epsilon\times10^6)$ psi vs width coordinate X at the 90/ − 30 interface of the laminate.

treated individually. In the second representation, the 0° layer is modeled as three different sublayers of equal thickness $h/3$. The third representation considers the 0° layer as three sublayers of $h/3$ thickness each and the 60° layer as two sub-layers, each of thickness $h/2$. The fact that the results by all the three representations of the laminate are the same show that these results are nearly exact.

Figure 4 shows the stress component σ_z for $(0/(\pm 60)_2)_s$-laminate by three different representations. For the first representation, the theory developed in [1] has been used and for the other two representations the present global–local model has been used. It has been seen that the results obtained by the middle representation, i.e. $(0H/0H/60/\overline{-60/60/-60})$ are nearly identical with those obtained by [1] for the same representation of the local domain. The values

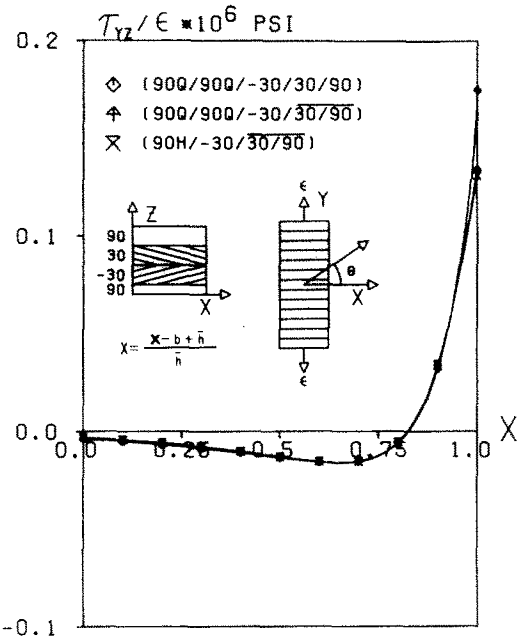

Fig. 9. Stress distribution $\tau_{yz}/(\epsilon \times 10^6)$ psi vs width coordinate X at the $90/-30$ interface of the laminate.

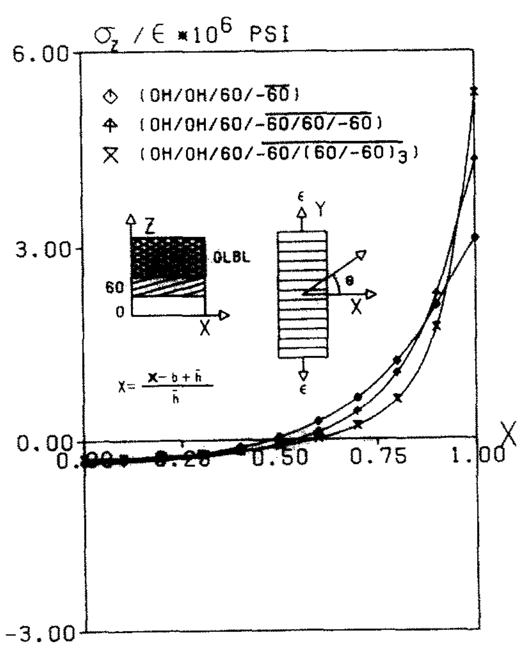

Fig. 10. Stress distribution $\sigma_z/(\epsilon \times 10^6)$ psi vs width coordinate X at the mid surface of the laminate.

obtained through the third representation only differ slightly from those for the other two cases. Further analysis shows that the "hump" is caused by insufficient subdivision of 0° layer, rather than the local-global model.

Figure 5 shows the variation of the stress component σ_z along x-axis for $(90H/\pm 30/90)_s$-laminate by three different representations. It is seen that the results obtained by the local-global models differ considerably from those obtained by model of [1]. The results by the third representation differ from those for the second representation adjacent to the free edge and are close elsewhere. Figure 6 shows more results for the same laminate. In this figure the third representation is the same as that of Fig. 5. Also in Fig. 6 we have used a different representation, $(90Q/90Q/-30/\overline{30/90})$, of the same laminate. In this case it has been found that the agreement between the [1] model results and the local-global model results is again quite good. Hence, an extra hump in the results by the third representation is likely due to insufficient subdivision of the inner 90° layer. This shows that another factor may be important in obtaining satisfactory results. The precise definition of this factor is not known presently, however, it appears that a gradual transition between the local and global regions may be helpful in obtaining accurate results, i.e. the middle representation of Fig. 6. Another factor involved in the results of Fig. 5 is that the computed stress component σ_z is of considerably lower magnitude as compared to that in the laminate of Fig. 4. Thus, the absolute magnitude of the error in the results for the first representation of Fig. 5 is small, although the relative error may be quite large. It can be seen from Fig. 7 that for the same ply representations as those in Fig. 5 the relative error in the results for $(90H/\mp 15/90)_s$-laminate is small as compared to that for $(90H/\mp 30/90)_s$-laminate. The results for $(90Q/90Q/-15/\overline{15/90})$ representation are also computed and are the same as those of the first representation of Fig. 7. Thus, it appears that the absolute magnitude of the stress component σ_z is also important in modeling the laminate representations for accurate results.

Figure 8 shows the stress component τ_{xz} at the $90/-30$ interface of a $(90H/\mp 30/90)_s$-laminate. As in the case of σ_z, the results by model [1] are nearly identical to those by the present model with $(90Q/90Q/-30/\overline{30/90})$ representation. The values computed through the other representation of the present model are slightly different from the others. However, the maximum value of τ_{xz} will increase with larger numbers of sublayers in the 90° ply. This is a characteristic of the general class of models being presented and is discussed in more detail in [1].

Figure 9 gives the stress component τ_{yz} for the aforementioned laminate at the $90/-30$ interface. In this case also, the comparison amongst the results by three different representations is reasonable, although an elastic singularity is expected in this stress component. Hence, again significant dependence on sublayer size will be present near the edge.

Figure 10 shows the stress component σ_z for $(0/(\pm 60)_n)_s$ $n = 1, 2, 4$ laminates as computed by the local-global model. The results given for the first two values of n, i.e. $n = 1, 2$, are already shown to be identical with those obtained by using [1], Fig. 3 and 4. The results for $n = 4$ show the expected trend. There exist no results in the open literature to compare with these values.

CONCLUSIONS

A self-consistent model has been developed to investigate the stress fields in laminated media consisting of numerous layers. The new model defines detailed response functions, such as interlaminar stresses and single layer forces and moments in a predetermined region of interest (local), while the remainder of the domain is represented by its effective material properties and the corresponding resultant forces and moments (global). The local model employs a theory [1] which approaches the theory of elasticity in the limit of vanishing layer thickness. The global model is based upon the theory given by Whitney and Sun [6] which has been demonstrated to produce good agreement with elasticity results on the global boundary for a particular laminate by Pagano [7]. While a particular arrangement of global and local domains has been considered here for brevity, there is no difficulty in extending these results to include more general arrangements, including the use of more than one global domain. The importance of the latter option follows from the observation that model accuracy may be improved by a gradual rather than abrupt transition of region.

The effectiveness of the model has been demonstrated by use of numerical examples based upon the free-edge class of boundary value problems in laminate elasticity. Preliminary results have been shown to be very promising although an apparent loss in accuracy occurs in the calculation of stress components of small magnitude, which may thus require finer subdivision of the local region than would normally be required. Similarly, the effect of the aforementioned "transition region" on model precision will require further study. These studies as well as the development of a solution schemes for fully three dimensional problems (which will depend only on two space variables in this theory), will be the subject of future investigations.

It is clear that theories of the type presented here are needed to describe the response of laminated structural components used in practice. However, experimental activity in this regard is vital, as proper interpretation of the field analysis, particularly in regions of very steep stress gradients, is needed to characterize initial failure and subsequent damage growth in these bodies.

Acknowledgement—The work reported herein was performed at the Nonmetallic Materials Division, Materials Laboratory, Air Force Wright Aeronautical Laboratories, Wright Patterson AFB, Dayton, Ohio.

REFERENCES

1. N. J. Pagano, Stress fields in composite laminates. AFML-TR-77-114, Wright Patterson Air Force Base, Dayton, Ohio, August 1977. Also, *Int. J. Solids Structures* **14**, 385 (1978).
2. M. E. Gurtin, Continuum theory of Fracture. *Mechanics of Composites Review*, p. 83. Bergamo Center, Dayton, Ohio (1977).
3. A. S. D. Wang and F. W. Crossman, Some new results on edge effect in symmetric composite laminates. *J. Composite Mat.* **11**, 92 (1977).
4. E. L. Stanton, L. M. Crain and T. F. Neu, A parametric cubic modelling system for general solids of composite material. *Int. J. Num. Meth. Engng* **11**, 653 (1977).
5. N. J. Pagano, Exact moduli of anisotropic laminates. In *Composite Materials, Mechanics of Composite Materials* (Edited by G. P. Sendecky), Vol. 2, pp. 23–44. Academic Press, New York (1974).
6. J. M. Whitney and C. T. Sun, A higher order theory for extensional motion of laminated composites. *J. Sound Vibr.* **30**, 85 (1973).
7. N. J. Pagano, On the calculation of interlaminar normal stress in composite laminate. *J. Composite Mat.* **8**, 65 (1974).
8. N. J. Solomon, An assessment of the interlaminar stress problem in laminated composites. *J. Composite Matl. Supplement* **14**, 177 (1980).
9. R. L. Spilker and T. C. T. Ting, Stress analysis of composites. Army Materials and Mechanics Research Center, Watertown, Mass. Techn. Rep. AMMRC-TR-81-5, 1981.
10. I. S. Raju, J. D. Whitcomb and J. G. Goree, A new look at numerical analyses of free edge stresses in composite laminates. NASA Tech. Paper 1751, 1981.
11. N. N. Blumberg and V. P. Tamuzh, Edge effects and stress concentrations in multilaminate composite plates. *Mechanics of Composite Materisls*, pp. 298–307 (1980). Translated from Russian *Jl. Mekh. Kompositn. Mater.* 3, 424 (1980).
12. V. V. Partsevskii, Approximate analysis of mechanisms of fracture of laminated composites at a free edge. *Mechanics of Composite Materials*, pp. 179–185 (1980). Translation from Russian *Jl. Mekh. Kompositn. Mater.* **2**, 246 (1980).
13. N. J. Pagano and R. B. Pipes, Some observations on the interlaminar strength of composite laminates. *Int. Mech. Sci.* **15**, 679 (1973).
14. N. J. Pagano, Free edge stress fields in composite laminates. *Int. J. Solids Structures* **14**, 401 (1978).
15. M. A. Jenkins and J. F. Traub, A three stage variable-shift interation for polynomial zeros and its relation to generalized Rayleigh iteration. *Numerische Mathematik* **14**, 252 (1970).
16. M. Knight and N. J. Pagano, The determination of interlaminar moduli of graphite/epoxy composites. *Seventh Annual Mechanics of Composites Review*, AFWAL/NASA/NAVY/ARMY, Dayton Ohio, 28–30, Oct. 1981.